Dalton Transactions

Cite this: *Dalton Trans.*, 2011, **40**, 9123

www.rsc.org/dalton

PAPER

Synthesis, structure and photophysical properties of binuclear methylplatinum complexes containing cyclometalating 2-phenylpyridine or benzo{h}quinoline ligands: a comparison of intramolecular Pt–Pt and π–π interactions†

Sirous Jamali,*[a] Rafal Czerwieniec,[b] Reza Kia,[c] Zahra Jamshidi[d] and Manfred Zabel[e]

Received 4th May 2011, Accepted 10th June 2011
DOI: 10.1039/c1dt10834d

The binuclear cyclometalated complexes $[Pt_2Me_2(ppy)_2(\mu\text{-dppm})]$, **1a**, and $[Pt_2Me_2(bhq)_2(\mu\text{-dppm})]$, **1b**, in which ppy = 2-phenylpyridyl, bhq = benzo{h}quinoline and dppm = bis(diphenylphosphino)-methane, were synthesized by the reaction of $[PtMe(SMe_2)(ppy)]$ or $[PtMe(SMe_2)(bhq)]$ with 1/2 equiv of dppm at room temperature, respectively. Complexes **1a** and **1b** were fully characterized by multinuclear (^1H, ^{31}P, ^{13}C, and ^{195}Pt) NMR spectroscopy and were further identified by single crystal X-ray structure determination. A comparison of the intramolecular Pt–Pt and π–π interactions in complexes **1a** and **1b** has been made on the basis of data on crystal structures and wave functions analysis. The binuclear complexes **1a** and **1b** are luminescent in the solid state, and showing relatively intense orange–red emissions stemming from ^{3}MMLCT excited states. The reaction of complex **1b** with excess MeI gave the binuclear cyclometalated Pt(IV)–Pt(IV) complex $[Pt_2Me_4(bhq)_2(\mu\text{-}I)_2]$, **2**. Crystal structure of complex **2** shows intermolecular C–H···I and C–H···π interactions in solid state.

Introduction

Among the growing collection of transition metal complexes under consideration for optoelectronic device applications, cyclometalated platinum complexes show great attention because of their rich luminescence properties.[1] The ability of coordinatively unsaturated cyclometalated platinum(II) complexes to substrate-binding has been proved, and these contacts usually bring a significant change in physical and chemical properties of these complexes. For example, weak interactions such as metal–metal and ligand–ligand (π–π) interactions are important strategies used for assembling cyclometalated platinum complexes into luminescent nanostructures.[2] In many Pt(II) complexes with cyclometallating ligands the emission originates from the lowest MLCT-perturbed ligand-centered ^{3}LC excited state. The planar geometry of molecules of these d^8 complexes often leads to strong intermolecular Pt–Pt interactions.[3] As a result, prominent red shifts of the luminescence are observed in dimers or in column-type agglomerates. Cyclometalated platinum(II) complexes can be highly reactive *via* oxidative addition to give the corresponding platinum(IV) products. Oxidative addition reactions of reactive and less reactive substrates to cyclometalated platinum(II) complexes have been carried out and many cyclometalated platinum(IV) complexes have been prepared *via* intramolecular oxidative addition of C–X bond.[4,5] These reactions have also been used as a probe in phosphorescence-based sensing systems for cyanogen halides.[6]

A series of cyclometalated platinum(II) complexes of the types $[Pt_2R_2(C\text{^}N)_2(\mu\text{-dppf})]$, $[Pt_2R_2(C\text{^}N)_2(\mu\text{-dppm})]$ and $[Pt_2R_2(C\text{^}N)_2(\mu\text{-dppe})]$, in which, dppf = 1,1′-bis(diphenylphosphino)ferrocene (R = Me or aryl), dppm = bis(diphenylphosphino)methane (R = aryl), dppe = bis(diphenylphosphino)ethane (R = Me or aryl) and C^N = ppy (ppyH = 2-phenylpyrine) or bhq (bhq = benzo{h}quinoline) ligands have recently been prepared.[7] These compounds are binuclear platinum complexes containing an open bridge bisphosphine ligand with an antiperiplanar staggered conformation in which the two PtR(C^N) subunits are well separated and so no intramolecular Pt–Pt or π–π interactions are observed. It seems that the presence of sterically bulky aryl and bisphosphine ligands prevented two platinum(II) centers from coming into close proximity. In continuation of our interest in binuclear cyclometalated Pt(II) complexes, in this study we report the preparation and characterization of new binuclear cyclometalated methylplatinum(II) analogous complexes $[Pt_2Me_2(ppy)_2(\mu\text{-dppm})]$, **1a**, and $[Pt_2Me_2(bhq)_2(\mu\text{-dppm})]$, **1b**. We have observed that the presence of the small bite angle ligand dppm in methylplatinum analogues brings about some interesting changes in the molecular structures and photophysical properties.

[a]*Chemistry Department, Sharif University of Technology, Tehran, P.O. Box 11365-9516, Iran. E-mail: sjamali@sharif.ir*
[b]*Universität Regensburg, Institut für Physikalische und Theoretische Chemie, Regensburg, Germany*
[c]*Department of Chemistry, Science and Research Branch, Islamic Azad University, Tehran, Iran*
[d]*Chemistry and Chemical Engineering Research Center of Iran, Tehran, Iran*
[e]*Universität Regensburg, Institut für Anorganische Chemie, Zentrale Analytik, Regensburg, Germany*

† CCDC reference numbers 814825–814827. For crystallographic data in CIF or other electronic format see DOI: 10.1039/c1dt10834d

One of the most remarkable features of halide ligands (M–X) is their tendency to act as hydrogen bond acceptors.[8] Although the C–H···X–M interactions are weaker than conventional H-bonds involving O and/or N atoms, in the absence of any other stronger intermolecular interactions weak hydrogen bonds can be used to direct crystal designs. Indeed, many supramolecular synthons based upon weak hydrogen bonds have been identified[9] and the construction and understanding of structures using these interactions incorporated into many topical areas of research such as materials and organometallic chemistry.[10] Reaction of the binuclear complex **1b** with excess MeI gave a mixture of binuclear Pt(IV)–Pt(IV) complexes that eventually converted to the binuclear Pt(IV)–Pt(IV) complex $[Pt_2Me_4(bhq)_2(\mu\text{-}I)_2]$, **2**, by dissociation of dppm ligand. Complex **2** was shown to display a 1-D extended chain arrangement through C–H···I hydrogen bonds in solid state along the *a*-axis of the unit cell.

Results and discussion

Synthesis and structural characterization

The routes to prepare the cyclometalated organoplatinum complexes are described in Scheme 1. The reaction of a yellow solution of either $[PtMe(SMe_2)(ppy)]$ or $[PtMe(SMe_2)(bhq)]$ with 0.5 equiv of dppm at room temperature gave the binuclear complexes $[Pt_2Me_2(ppy)_2(\mu\text{-dppm})]$, **1a**, or $[Pt_2Me_2(bhq)_2(\mu\text{-dppm})]$, **1b**, respectively, in good yields by replacement of SMe_2 ligands with the P ligating atoms of dppm. Complexes **1a** and **1b** are air-stable orange to red solids that are stable in acetone or chloroform solutions for several hours. The complexes **1a** and **1b** were fully characterized by multinuclear ^1H, ^{31}P, ^{13}C, and ^{195}Pt NMR spectroscopy. In the ^{31}P NMR spectra (see Fig. 3(i) for **1b**) of complexes **1a** and **1b**, the two equivalent phosphorus atoms of dppm resonated as singlet signals at $\delta = 20.8$ and 20.4 ppm and showed short range coupling platinum satellites with $^1J_{PtP} = 2080$ and 2117 Hz as well as platinum satellites arising from long range couplings with $^3J_{PtP} = 35$ and 46 Hz, respectively. Consistently, the ^{195}Pt NMR spectra of complexes **1a** and **1b**, showed doublet of doublet signals at $\delta = -2520$ and -2563 ppm that are due the short range coupling of each platinum with one phosphorus atom directly connected to the platinum with $^1J_{PtP} = 2150$ and 2129 Hz which further couples to the distant P atom of dppm ligand with $^3J_{PtP} = 48$ and 43 Hz, respectively. In the ^1H NMR spectra of complexes **1a** and **1b**, the Me ligands, located symmetrically as shown in Scheme 1, appeared as doublets at δ 0.82 and 1.02 ppm due to coupling with the phosphorus atoms with $^3J_{PH} = 7.5$ and 5 Hz that is further coupled to Pt atoms with $^2J_{PtH} = 83$ and 79 Hz. This was confirmed by the observation of doublet signals in the

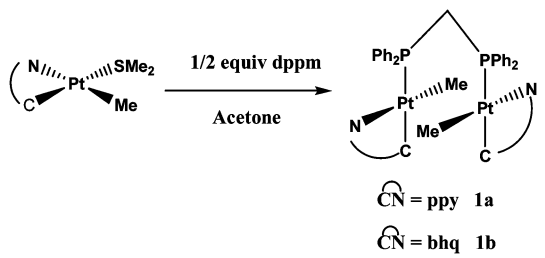

Scheme 1

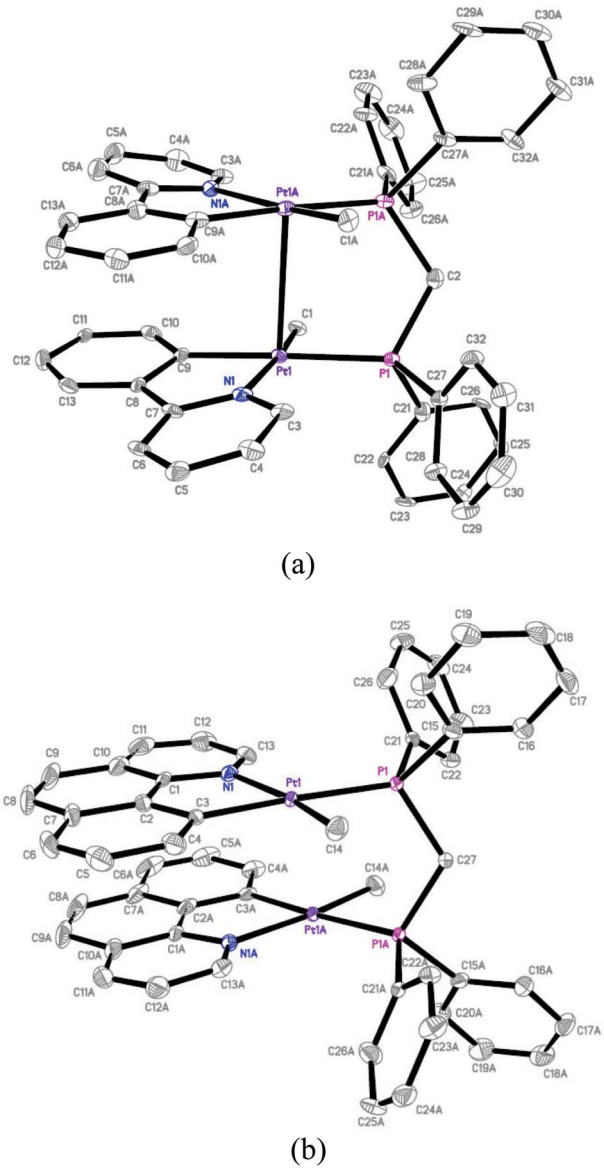

Fig. 1 The molecular structure of complexes **1a** and **1b**, showing 30% probability displacement ellipsoids and the atomic numbering. The suffix A in **1b** corresponds to symmetry code $(1 - x, -y, 1 - z)$. Hydrogen atoms as well as CH_2Cl_2 solvent molecule (in **1b**) were omitted for clarity.

^{13}C NMR spectra of complexes **1a** and **1b** at $\delta -10.9$ and -11.4 due to the equivalent Me groups with $^2J_{PC} = 5$ and 3 Hz, respectively, indicating that the Me groups are situated *cis* to the phosphorus atoms; the signals give platinum satellites with $^1J_{PtC} = 715$ and 725 Hz, respectively. The other signals in the ^1H and ^{13}C NMR spectra appeared as expected (see the experimental section for the details). Two types of crystals were obtained by crystallization of **1b**. Block-like yellow and fine needle-like red crystals were formed by layering CH_2Cl_2 solutions of **1b** with diethyl ether and hexanes respectively, the latter ones were not suitable for X-ray structural determination.

A single crystal X-ray diffraction study could be carried out on block-like yellow crystals and the structure of **1b** was confirmed by X-ray crystallography method. A view of the structure of **1b** (yellow form) is shown in Fig. 1(b). The complex

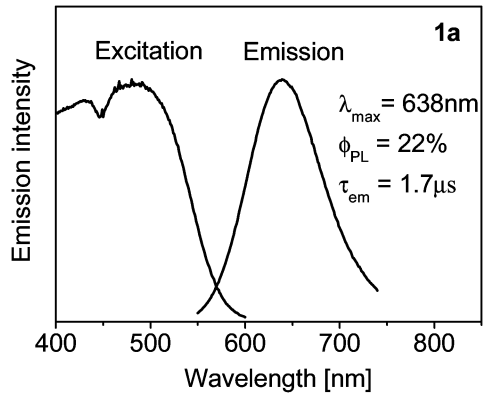

Fig. 2 Ambient temperature excitation and luminescence spectra of neat $[Pt_2Me_2(ppy)_2(\mu\text{-dppm})]$, **1a**. The excitation spectrum was detected at λ_{det} = 650 nm. Luminescence was measured upon excitation at λ_{exc} = 500 nm.

Table 1 Selected bond distances (Å) and angles (°) of **1a**, **1b** and **2**

Complex **1a**			
Pt1–Pt1A	3.1113(9)	C9–Pt1–C1	90.8(4)
Pt1–P1	2.271(2)	C9–Pt1–N1	80.3(4)
Pt1–N1	2.093(10)	C1–Pt1–N1	170.1(4)
Pt1–C1	2.042(11)	C9–Pt1– P1	174.2(3)
Pt1–C9	2.041(9)	C1–Pt1–P1	84.2(3)
		N1–Pt1–P1	104.4(3)
Complex **1b**			
Pt1–Pt1A	3.763	P1–Pt1–N1	105.31 (8)
Pt1–P1	2.2889 (9)	P1–Pt1–C3	174.65(10)
Pt1–C14	2.059 (3)	P1–Pt1–C14	86.56(10)
Pt1–N1	2.136 (3)	N1–Pt1–C3	80.03(12)
Pt1–C3	2.040(3)	N1–Pt1–C14	168.07(13)
		N1–Pt1–C14	88.11(14)
Complex **2**			
Pt1–I1	2.7902(8)	I1–Pt1–N1	87.8(3)
Pt1–I1A	2.7589(9)	I1–Pt1–C11	93.3(3)
Pt1–N1	2.156(10)	I1–Pt1–C14	178.4(4)
Pt1–C11	1.998(11)	I1–Pt1–C15	93.0(4)
Pt1–C14	2.080(13)	N1–Pt1–C11	81.7(4)
		N1–Pt1–C14	91.1(5)
		N1–Pt1–C15	174.6(4)

crystallizes in a monoclinic system with a *C*2/*c* space group. The molecule of the title complex lies across a crystallographic twofold rotation axis which passes through the C27 atom of the dppm ligand. The geometry around the Pt centre is a distorted square-planar. However, compared to arylplatinum analogues where the dppm ligand adopts an anti conformation such that the two square-planar platinum centers are well separated [Pt(1)···Pt(2) = 6.73 Å] and allows intermolecular π–π interaction of bhq groups,[7b,c] the structure of **1b** shows a bent conformation with the Pt(bhq)(CH_3)(PPh_2) subunits situated face-to-face. For **1b** (yellow form), the intramolecular Pt–Pt distance is 3.7628(2) Å which indicates weak interactions between Pt1–Pt2 in solid state. The two [(bhq)Pt] units are partially staggered, with torsion angles of 9° about the Pt1–Pt1A axes (defined by the angle between the C9A–Pt1–Pt1A and N1–Pt1–Pt1A planes), which shows this nearly parallel face to face conformation, supported by intramolecular π–π interactions with centroid to centroid distances of 3.542(2)–3.7041(17) Å. The X-ray crystal structure of **1a** was also determined, and a view of the structure of the complex is shown in Fig. 1(a). The structure of **1a** shows a bent conformation similar to that for complex **1b**. The two [(ppy)Pt] units in complex **1a** are staggered, with torsion angles of 36° about the Pt1–Pt1A axes (defined by the angle between the C9A–Pt1–Pt1A and N1–Pt1–Pt1A planes) such that the π–π interaction between ppy ligands in **1a** is smaller than that between bhq ligands in **1b**. However, compared to that of **1b**, the metal–metal interaction in **1a** is improved significantly and the chelate ring of a PtMe(ppy) unit makes an intramolecular π–π-stacking interaction with the aryl ring of the ppy ligand on the other unit at an average centroid to centroid distance of 3.675(6) Å and an offset of 3.445(5) Å along the *a*-axis of the unit cell. Further examination of the crystal structure of **1a** reveals that the molecule has weak intramolecular edge-to-face C–H···π interactions [dC–H···C = 3.494(13) and 3.515(10) Å], between the phenyl rings [C27–C32 and C8–C13] of the dppm ligand and the protons [C3–H3A and C24–H24A] of the ppy ligands, respectively. The Pt–Pt distance in **1a** is 3.1113(9) Å, which is significantly shorter than the value of 3.7628(2) Å in **1b** and falls within the range of intermetal distances (3.09–3.50 Å) observed in monomeric Pt(II) linear-chain structures.[11] Selected bond distances and angles are given in Table 1. Wave function analysis based on QTAIM calculations show excellent agreement with results of the crystallography experiments. Topological analysis of the electron density has been carried out at the crystal geometry of the complexes **1a** and **1b** (using B3LYP method and all electron WTBS basis set for Pt and 6-31+G(d,p) basis set for H, C, O, N, and P atoms) to identify the presence of weak interaction through the existence of bond path connecting the bonded atoms. The value of the electron density $\rho(r)$ at the bond critical points (BCPs) can be correlated to the bond strength, bond length and also bond order. A comparison of the Pt–Pt interaction stability in complexes **1a** and **1b** has been made by computing the maximum value of electron density through the Pt–Pt bond path. The electron density at the Pt–Pt bond critical point is significantly bigger for **1a** (2.5×10^{-2} au) than for **1b** (0.9×10^{-2} au) which can be related to the binding energy trends. The Wiberg bond order[12] for the Pt–Pt bond is 0.023 and 0.008 for complexes **1a** and **1b**, respectively and correlated with the bond length and electron density values. In both complexes we can find the bond paths that show π–π interaction between the phenylpyridine and benzo{h}quinoline rings. The number of bond paths connected between ppy ligands in complex **1a** and bhq ligands in complex **1b** is 4 and 6, respectively, and the values of electron density in the BCPs are in the range 0.5×10^{-2}–0.6×10^{-2} au. It has been suggested that a bond critical point with a $\rho(r)$ of ~0.006 au can be associated with a bond energy of ~1 kcal mol^{-1}. A cumulative effect of several such interactions leads to a non-negligible stabilization energy.[13] However when the sum of the $\rho(r)$ of all the π–π interactions BCPs is considered, the total value is about 2.2×10^{-2} au (between ppy rings in **1a**) and 3.5×10^{-2} au (between bhq rings in **1b**). It seems that there is a competition between Pt–Pt and π–π interactions in these two complexes, such that twisting of the flexible ppy ligands in **1a** promotes a decrease in the π–π interaction between ppy ligands and an increase in the Pt–Pt interaction. In contrast, the rigid bhq ligands in **1b** are capable of assembling the two [(bhq)Pt] units in a face-to-face manner with an increasing π–π interaction between bhq ligands and simultaneously suppressing the intramolecular Pt–Pt interaction.

Table 2 Luminescence properties of neat **1a** and **1b**

	λ_{max} [nm][a]	φ_{PL} [%][b]	τ_{em} [μs][c]
1a	638	22	1.7
1b	655	15	1.2

[a] Emission maximum, error ± 1 nm, [b] Photoluminescence quantum yield, error ± 2%, [c] Emission decay time measured at λ_{det} = 640 nm (**1a**) or 660 nm (**1b**), error ± 0.2 μs

Luminescence properties of the dinuclear Pt(II) complexes

The binuclear complexes $[Pt_2Me_2(ppy)_2(\mu\text{-dppm})]$, **1a**, and $[Pt_2Me_2(bhq)_2(\mu\text{-dppm})]$, **1b**, are brightly luminescent in the solid state. The emission and excitation spectra of neat $[Pt_2Me_2(ppy)_2(\mu\text{-dppm})]$, **1a**, are shown in Fig. 2 and the photophysical data of **1a**, and **1b** listed in Table 2. Both complexes **1a** and **1b** show broad structureless emission bands centered at λ_{max} = 638 and 655 nm, respectively. The photophysical behaviour of neat $[Pt_2Me_2(ppy)_2(\mu\text{-dppm})]$, **1a**, and $[Pt_2Me_2(bhq)_2(\mu\text{-dppm})]$, **1b**, differs distinctly from that of the mononuclear Pt(II) complexes containing cyclometallating ppy or bhq ligands. For example, the lowest energy absorption (associated with the $S_0 \rightarrow {}^1$MLCT electronic transition) in the complex [Pt(ppy)(acac)], in which acac = acetylacetonate, occurs at $\lambda_{abs} < 450$ nm. In 2-methyltetrahydrofurane solution this complex displays intense green luminescence with a maximum at 486 nm.[14] The emission spectrum of [Pt(ppy)(acac)] shows a partly preserved vibronic structure even at ambient temperature. It has been attributed to a spin forbidden $S_0 \leftarrow T_1$ transition, from the lowest triplet state T_1, which represents a ligand(ppy) centered ^{3}LC state perturbed (*via* spin–orbit coupling) by higher lying ^{1}MLCT states.[15] Similar behaviour can be expected for the complexes [Pt(bhq)(Me)(phosphine)] and [Pt(ppy)(Me)(phosphine)]. The lowest-energy electronic transitions of **1a** and **1b** are strongly red-shifted from the transitions of the related mononuclear complexes. The lowest absorption and the luminescence bands of neat **1a** and **1b** (see Fig. 2 for **1a**) occur at about 500 nm and at λ_{max} = 638, 655 nm, respectively. Similar effects were observed for the bi- or trinuclear Pt(II) complexes with bridging pyrazolyl and di/oligo-phosphine ligands.[3] The luminescence of such compounds was associated with the $^3[d\sigma_{Pt-Pt^*},\pi^*]$ (or ^{3}MMLCT) excited states and the low energy absorptions of **1a** and **1b** in solid state are assigned to transitions from the ground to the ^{1}MMLCT excited states.

Reaction of complex 1b with MeI

When the binuclear complex $[Pt_2Me_2(bhq)_2(\mu\text{-dppm})]$, **1b**, was reacted with excess MeI, as described in Scheme 2, a Pt(II)–Pt(IV) complex, suggested to have the structure **A**, was formed first by the reaction of MeI with one of the Pt(II) centers of the complex **1b**. MeI was further reacted with complex **1b** to give an almost 1 : 1 mixture of two Pt(IV)–Pt(IV) complexes, suggested to have structures **B** and **C**. When the latter mixture in acetone was allowed to crystallized by vapour diffusion of ether, the very stable Pt(IV)–Pt(IV) complex $[Pt_2Me_4(bhq)_2(\mu\text{-}I)_2]$, **2**, was gradually formed during which the iodine ligands bridged between the Pt centers at the expense of complete removal of the dppm bridging ligand. Complex **2** was eventually separated as a white solid after a week. Reaction of **1b** with excess MeI was monitored by ^{31}P

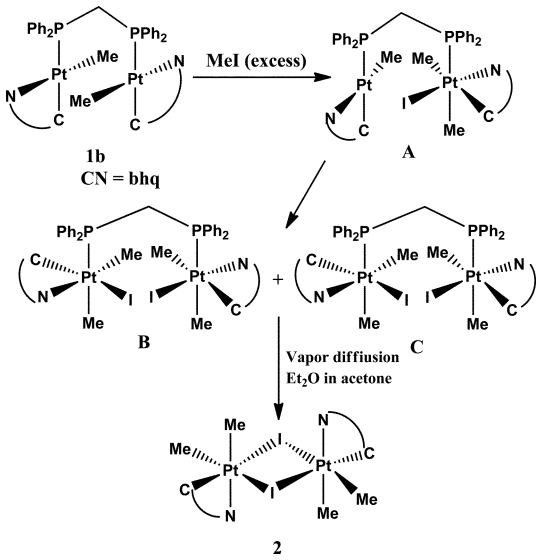

Scheme 2

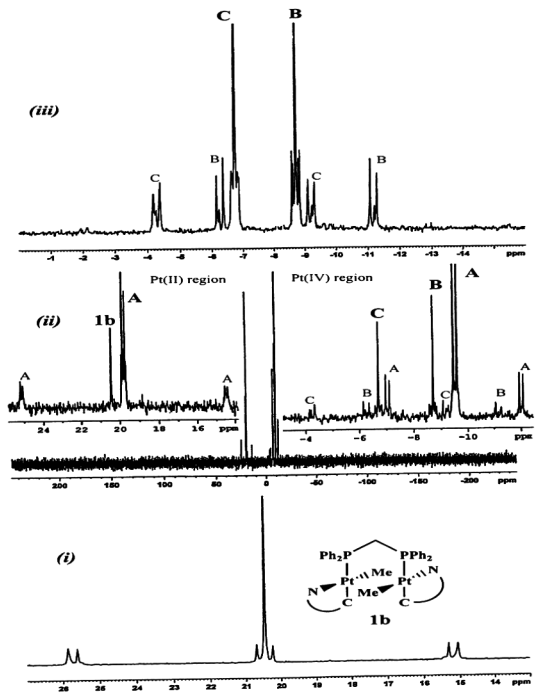

Fig. 3 ^{31}P NMR spectrum at room temperature of i) complex **1b**; ii) obtained 5 min after addition of excess MeI; iii) after 3 h.

NMR spectroscopy as shown in Fig. 3. Thus, right after the addition of excess MeI to complex $[Pt_2Me_2(bhq)_2(\mu\text{-dppm})]$, **1b**, the intermediate Pt(II)–Pt(IV) complex, **A**, was mainly formed along with a small amount of the mixture of complexes **B** and **C** and a trace amount of the unreacted starting complex **1b**. After 3 h the reaction gave a pure mixture of complexes **B** and **C**. For the phosphorus atom connected to the Pt(II) center of intermediate complex **A**, a signal was observed at δ = 19.8 as a doublet due to coupling with the phosphorus atom connected to the Pt(IV) center with $^2J_{PP}$ = 26 Hz; the signal also displays short range and long range couplings with the Pt centers with $^1J_{PtP}$ = 2158 Hz and $^3J_{PtP}$ = 25 Hz. These parameters are very close to the values obtained for

Table 3 Crystal data and structure refinement parameters for **1a**, **1b** and **2**

Complex	**1a**	**1b**	**2**
Empirical formula	$C_{98}H_{88}N_4P_4Pt_4$	$C_{53}H_{44}N_2Pt_2$, CH_2Cl_2	$C_{30}H_{28}I_2N_2Pt_2$
Formula weight	2225.96	1245.94	1060.50
Crystal size (mm)	0.02 × 0.11 × 0.14	0.11 × 0.18 × 0.20	0.04 × 0.05× 0.50
Colour	Orange	Yellow	White
Crystal system	Triclinic	Monoclinic	Orthorhombic
Space group	$P\bar{1}$	$C2/c$	$Pbca$
θ_{max} (°)	62.09	31.45	29.2
a (Å)	9.5031 (19)	15.9793(2)	6.8451(5)
b (Å)	11.957(2)	18.5039(2)	19.914(2)
c (Å)	18.978(4)	15.2131(2)	20.9767(16)
α (°)	101.34	90	90
β (°)	90.10(3)	90.463(1)	90
γ (°)	109.02(3)	90	90
V (Å^3)	1996.9(7)	4498.05(10)	2859.4(4)
Z	2	4	4
d_c (Mg m^{-3})	1.851	1.839	2.464
μ (mm^{-1})	13.956	13.541	11.955
F(000)	1076	2411	1936
Index ranges	$-10 \le h \le 10$	$-18 \le h \le 18$	$-9 \le h \le 6$
	$-13 \le k \le 13$	$-21 \le k \le 20$	$-20 \le k \le 27$
	$-21 \le l \le 21$	$-17 \le l \le 17$	$-25 \le l \le 28$
No. of collected reflections	6658	36 418	10 484
No. of independent reflections/ R_{int}	3044/0.0502	3617/0.029	3843/0.091
No. of obs. reflns. $I > 2\sigma(I)$	2461	3544	3278
No. of parameters	498	286	166
GOF	0.99	1.09	1.04
R_1 (observed data)	0.036	0.0212	0.0870
wR_2 (all data)[a]	0.0881	0.0530	0.1961

[a] $w = 1/[\sigma^2(F_o^2P)^2 + (0.0665P)^2]$ for **1a** $w = 1/[\sigma^2(F_o^2P)^2 + (0.0267P)^2 + 29.3349P]$ for **1b** and $w = 1/[\sigma^2(F_o^2) + (0.1805P)^2 + 35.0335P]$ for **2**, where $P = (F_o^2 + 2F_c^2)/3$

the starting binuclear Pt(II) complex **1b** (see above). The signal for the phosphorus atom connected to the Pt(IV) center was observed further up field as a doublet at $\delta = -9.5$ with $^2J_{PP} = 27$ Hz which again has short range and long range couplings with the Pt centers with $^1J_{PtP} = 1007$ Hz and $^3J_{PtP} = 25$ Hz, and the parameters are very close to the values obtained for phosphorus atoms of the Pt(IV)–Pt(IV) complexes **B** and **C**, see below. The signals for the mixture of complexes **B** and **C** can clearly be observed in Fig. 3(iii). The resonances which appeared at $\delta = -6.7$ (with $^1J_{PtP} = 998$ Hz, $^3J_{PtP} = 6$ Hz, and $^2J_{PP} = 41$ Hz) and at $\delta = -8.7$ (with $^1J_{PtP} = 998$ Hz, $^3J_{PtP} = 9$ Hz, and $^2J_{PP} = 43$ Hz) were assigned to the two symmetrical Pt(IV)–Pt(IV) dimers **B** and **C**, in each of which the two phosphorus atoms are equivalent. The final complex **2** was very insoluble and was characterized by single crystal X-ray analysis as described below. Vapour diffusion of ether into an acetone solution of a mixture of complexes **A** and **B** gave single crystals of complex **2** suitable for X-ray analysis. The crystal data and the details of the refinement are summarized in Table 3.

Selected bond distances and angles are given in Table 1 and Fig. 4 gives a perspective view of the dimeric Pt(IV)–Pt(IV) complex $[Pt_2Me_4(bhq)_2(\mu\text{-}I)_2]$, **2**, which lies across the crystallographic inversion centre. Each platinum center has a distorted octahedral geometry which is coordinated by the methyl groups, bhq ligands, and bridging iodo ligands. The dihedral angle between the mean plane of the two symmetry-related bhq is 0.0(2)°. The Pt1–I1 distance [2.7902(8) Å] is longer than the Pt1–I1A distance [2.7589(9) Å], which shows the *trans* effect of the terminally coordinated methyl group (C15) is stronger than the C11 atom of the bhq ligand. Interesting intermolecular C1–H1···I1 [3.677(12) Å;

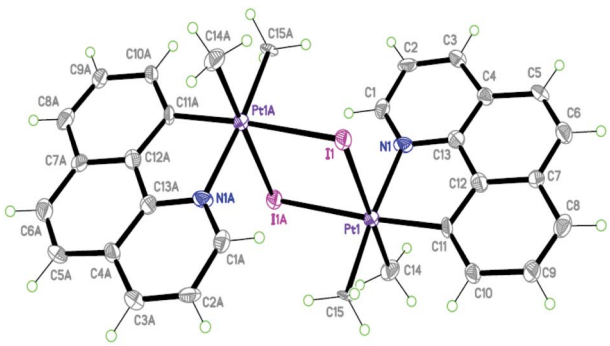

Fig. 4 The molecular structure of complex **2**, showing 50% probability displacement ellipsoids and the atomic numbering. The suffix A corresponds to symmetry code ($-x$, y, $0.5 - z$).

symmetry code: $1-x$, $-y$, $1-z$] H-bond interactions have been observed in the crystal structure of complex **2** producing $R^2_2(10)$ ring motifs. These interactions along with the intermolecular C–H···π interactions [$d_{C\text{–}H\cdots C}$ = 3.572(14) and 2.706(15) Å] between the phenyl rings [C7–C12 and Pt1/N1/C13/C12/C11] of the benzo{h}quinoline ligand, link neighbouring molecules into a 1-D extended chain along the a-axis of the unit cell, Fig. 5.

Experimental

The ^{1}H, ^{13}C, ^{31}P and ^{195}Pt NMR spectra were recorded on a Bruker Avance DRX 500-MHz spectrometer. The operating frequencies and references, respectively, are shown in parentheses

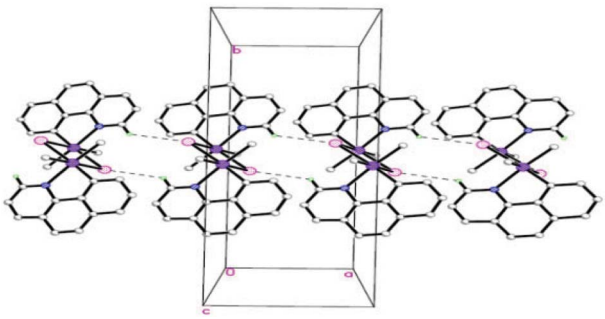

Fig. 5 The crystal packing of complex **2**, viewed down the *a*-axis showing linking of molecules into a 1-D extended chain along the *a*-axis through intermolecular C–H···I interactions (dashed lines).

as follows: ^{1}H (500 MHz, TMS), ^{13}C (125 MHz, TMS), ^{31}P (202 MHz, 85% H_3PO_4), and ^{195}Pt (107 MHz, aqueous Na_2PtCl_4). The chemical shifts and coupling constants are in ppm and Hz, respectively. 2-Phenylpyridine, benzo{h}quinoline and bis(diphenylphosphino)methane were purchased from Aldrich and $[Pt(\mu\text{-}SMe_2)Me_2]_2$ was prepared as described previously.[16] The complexes $[PtMe(SMe_2)(ppy)]$ and $[PtMe(SMe_2)(bhq)]$ were prepared *in situ* by the reaction of $[Pt(\mu\text{-}SMe_2)Me_2]_2$ with 2 equiv of 2-phenylpyridine or benzo{h}quinoline in acetone.[17]

$[Pt_2Me_2(ppy)_2(\mu\text{-dppm})]$, 1a

2-Phenylpyridine (100 µl, 0.7 mmol) was added dropwise *via* syringe to a solution of $[Pt(\mu\text{-}SMe_2)Me_2]_2$ (200 mg, 0.35 mmol) in 20 mL of acetone at room temperature in air. The solution immediately turned orange, and small bubbles formed. After stirring for 1.5 h, dppm (135 mg, 0.35 mmol) was added, and the solution was further stirred for 1 h. A bright orange–red solid was precipitated which was separated and dried under vacuum. Yield: 272 mg, 70%. Anal. Calcd for $C_{49}H_{44}N_2P_2Pt_2$: C, 52.8; H, 3.9; N, 2.5; Found: C, 52.5; H, 4.1; N, 2.6. NMR data in $CDCl_3$: $\delta(^{1}H)$ 0.82 (d, 6H, $^{2}J_{PtH}$ = 83.0 Hz, $^{3}J_{PH}$ = 7.5 Hz, 2 Me ligands), 4.08 (q, 2H, $^{3}J_{PtH}$ = 39 Hz, $^{2}J_{PH}$ = 9 Hz, CH_2 of dppm), 6.1 (m, 2H, CH groups adjacent to coordinated C atoms), 7–7.4 and 7.9 (m, 32H, overlapping multiplets of aromatic H atoms), 7.65 (m, 2H, $^{3}J_{PtH}$ = 49.5 Hz, CH groups adjacent to coordinated N atoms); $\delta(^{13}C)$ –10.9 (d, 2C, $^{1}J_{PtC}$ = 715, $^{2}J_{PC}$ = 5 Hz, 2Me ligands), 21.4 (t, 1C, $^{1}J_{PC}$ = 15.3 Hz, CH_2 of dppm), aromatic C atoms: 117 (s), 121 (s), 123.2 (s), 123.6 (s), 128 (m), 129 (d), 129.6 (s), 131 (s), 133 (m), 136 (s), 147 (s), 151 (s), 165.8 (d, $^{1}J_{PtC}$ not resolved $^{2}J_{PC}$ = 127 Hz, C atoms of the ppy ligands connected to Pt atoms); $\delta(^{31}P)$ 20.8 ($^{1}J_{PtP}$ = 2080 Hz, $^{3}J_{PtP}$ = 35 Hz, $^{2}J_{PP}$ = 31 Hz, 2P of dppm). $\delta(^{195}Pt)$ –2520 (dd, $^{1}J_{PtP}$ = 2150 Hz, $^{3}J_{PtP}$ = 48 Hz, 2Pt).

$[Pt_2Me_2(bhq)_2(\mu\text{-dppm})]$, 1b

Following the above procedure, used to prepare complex **1a**, benzo{h}quinoline (125 mg, 0.7 mmol) was added to a solution of $[Pt(\mu\text{-}SMe_2)Me_2]_2$ (200 mg, 0.35 mmol). After stirring for 1.5 h, dppm (135 mg, 0.35 mmol) was added. A bright orange–red solid was precipitated which was separated and dried under vacuum. Yield: 305 mg, 75%. Anal. Calcd for $C_{53}H_{44}N_2P_2Pt_2$: C, 54.8; H, 3.8; N, 2.4; Found: C, 54.3; H, 4.2; N, 2.5. NMR data in $CDCl_3$: $\delta(^{1}H)$ 1.02 (d, 6H, $^{2}J_{PtH}$ = 79 Hz, $^{3}J_{PH}$ = 5 Hz, 2 Me ligands); 4.3 (m, 2H, $^{2}J_{PH}$ = 9 Hz, CH_2 dppm); 5.9 (m, 2H, CH groups adjacent to coordinated C atoms); 6.9–7.4 and 7.9 (m, 32H, overlapping multiplets of aromatic H atoms); 7.7 (m, 2H, $^{3}J_{PtH}$ = 49.1 Hz, CH groups adjacent to coordinated N atoms); $\delta(^{13}C)$ –11.4 (d, 2C, $^{1}J_{PtC}$ = 725 Hz, $^{2}J_{PC}$ = 3 Hz, 2Me ligands), 20.2 (t, 1C, $^{1}J_{PC}$ = 16 Hz, CH_2 dppm); aromatic carbons: 120 (s); 122 (s); 122.7 (s); 125.5 (s); 128 (m); 128.4 (s); 128.5 (s); 129.5 (s); 133 (m); 134 (s); 135 (d); 143 (s); 150 (s); 154 (s); 162.9 (d, $^{1}J_{PtC}$ not resolved $^{2}J_{PC}$ = 129 Hz, C atoms of the bhq ligands connected to Pt atoms); $\delta(^{31}P)$ 20.4 ($^{1}J_{PtP}$ = 2117 Hz, $^{3}J_{PtP}$ = 46 Hz, $^{2}J_{PP}$ = 52 Hz, 2P of dppm); $\delta(^{195}Pt)$ –2563 (dd, $^{1}J_{PtP}$ = 2129 Hz, $^{3}J_{PtP}$ = 43 Hz, 2Pt).

Reaction of complex 1b with MeI

An excess of MeI (50 µL) was added to a solution of complex **1b** (100 mg in 20 mL of acetone) at 0 °C. The reaction mixture was further stirred at this condition for 1 h, then the solvent was removed under reduced pressure and the residue was triturated with ether (2 × 3 mL) and dried under vacuum. The product was characterized as a mixture of two complexes **B** and **C** and the components of the mixture were not isolable. NMR data for complex **B** in $CDCl_3$: $\delta(^{1}H)$ 1.01 (d, 6H, 3JPH = 7.5 Hz, $^{2}J_{PtH}$ = 59.3 Hz, Me ligands *trans* to P); 1.54 (d, 6H, $^{3}J_{PH}$ = 6.3 Hz, $^{2}J_{PtH}$ = 83 Hz, Me ligands *trans* to N), 4.1 (m, 1H, CH_2 dppm ligand); 5.2 (m, 1H, CH_2 dppm ligand); 6–8 (m, 36H, overlapping multiplets of aromatic H atoms); 9.9 (d, 2H, CH groups adjacent to coordinated N atoms); $\delta(^{31}P)$ –8 (s, $^{1}J_{PtP}$ = 955 Hz); NMR data for complex **C** in $CDCl_3$: $\delta(^{1}H)$ 1.07 (d, 6H, $^{3}J_{PH}$ = 7.2 Hz, $^{2}J_{PtH}$ = 61 Hz, Me *trans* to P); 1.25 (d, 6H, $^{3}J_{PH}$ = 7.5 Hz, $^{2}J_{PtH}$ = 72 Hz, Me *trans* to I); 4.45 (s, 2H, CH_2 dppm ligand), 6–8 (m, 36 H, overlapping multiplets of aromatic H atoms); 10.25 (d, 2H, CH groups adjacent to coordinated N atoms); $\delta(^{31}P)$ –9.5 (s, $^{1}J_{PtP}$ = 990 Hz, $^{3}J_{PtP}$ = 52 Hz). The reaction was monitored by ^{31}P NMR spectroscopy. Thus, excess MeI (2 drops) was added to a solution of **1b** (10 mg) in $CDCl_3$ in a sealed NMR tube and the spectra were obtained at room temperature. When an acetone solution containing the mixture of complexes **B** and **C** was allowed to crystallize by vapour diffusion of ether, decomposition occurred slowly to give crystals of complex **2** within a week. Yield: *ca.* 63%. Anal. Calcd. for $C_{30}H_{28}I_2N_2Pt_2$: C, 33.9; H, 2.6; N, 2.6; Found: C, 33.6; H, 2.5; N, 2.8. The complex was insufficiently soluble to allow NMR characterization.

Spectroscopic methods

Ambient temperature luminescence and excitation spectra were recorded with a Horiba Jobin Yvon Fluorolog 3 steady-state fluorescence spectrometer. This spectrometer was modified to allow for measurements of emission decay times. A pulsed diode laser (PicoQuant λ_{exc} = 375 nm, pulse duration 100 ps) was used as the excitation source. The emission was detected with a photomultiplier attached to a FAST ComTec multichannel scaler PCI card with a time resolution of 250 ps. Photoluminescence quantum yields were determined using a Hamamatsu system for absolute PL quantum yield measurements (type C9920-02) equipped with an integrating sphere with a Spectralon inner surface coating. All measurements were performed under a continuous flow of nitrogen gas in order to minimize emission quenching by oxygen.

Structural determination

Single crystals of these complexes were grown from slow diffusion of diethyl ether into saturated solutions of the complexes in dichloromethane (**1a**, **1b**) or slow diffusion of diethyl ether into an acetone solution of a mixture of complexes **A** and **B** (**2**). Suitable single crystals of complexes **1a**, **1b** (yellow form) and **2** were mounted on a glass fibers and all measurements were made on an Oxford diffraction Gemini Ultra diffractometer using Cu-Kα radiation, equipped with an Oxford cryosystem Cobra low temperature attachment (**1a**, **1b**), using Cu-Kα radiation or a STOE IPDS II diffractometer with graphite monochromated Mo-Kα radiation(2). Crystal data and refinement parameters for **1a**, **1b** and **2** are given in Table 3. The selected bond lengths and angles are listed in Table 1. For complexes **1a** and **1b**, the data collection, cell refinement and reduction, including the multi-scan absorption correction,[18] were performed using the *CrysAlis* software package.[19] The structures of **1a** and **1b** were solved by direct method (*SIR97*)[20] and refined by the least-squares refinement on F^2 using the *SHELXL97* program.[21] For the molecular graphics the program *SHELXTL*[21] was used. For complex **2**, the data collection, cell refinement and reduction, including the numerical absorption correction, was performed using the *X-AREA* 1.31 software package.[22] The structure was solved by direct method (*SHELXS97*)[21] and refined by the least-squares refinement on F^2 using the *SHELXL97*. All of the hydrogen atoms of complexes **1a**, **1b** and **2** were positioned geometrically and constrained with a riding model approximation with U_{iso}(H) = 1.2 or 1.5 U_{eq}(C).

Conclusions

Compared to previously reported analogous cyclometalated complexes,[7] the binuclear complexes **1a** and **1b** have a bent conformation and show intramolecular Pt–Pt and π–π interactions in solid state. Both compounds are strongly luminescent, with the emissions originating from the ^{3}MMLCT excited states. Evidence from the present study indicates that the flexible cyclometalating 2-phenylpyridine ligand improved intramolecular Pt–Pt and C–H···π interactions compared to benzo{h}quinoline in the binuclear platinum(II) systems. In contrast, the benzo{h}quinoline ligand can position two [(bhq)Pt] units into a face-to-face configuration and favours the intramolecular π–π interaction. When the binuclear complex **1b**, was reacted with excess MeI, based on the observations, a double oxidative addition of MeI occurred. However, the structure of the final product dimer Pt(IV)–Pt(IV) complex **2**, as determined by X-ray crystallography, indicated that the bridging dppm ligand was displaced by bridging iodide ligands. It seems that steric effects in bulky binuclear complexes **B** and **C** are responsible for the observed replacement of dppm by the bridging iodide ligands.

Acknowledgements

Financial support of Sharif University of Technology and Iran National Science Foundation (Grant No. 89000977) is gratefully acknowledged. SJ thanks Professor Mehdi Rashidi for many good discussions and preparation of the manuscript.

Notes and references

1 (*a*) H. Yersin, *Highly Efficient OLEDs with Phosphorescent Materials*; Wiley–VCH, Weinheim 2008; (*b*) W. B. Connick and H. B. Gray, *J. Am. Chem. Soc.*, 1997, **119**, 11620; (*c*) M. Hissler, J. E. McGarrah, W. B. Connick, D. K. Geiger, S. D. Cummings and R. Eisenberg, *Coord. Chem. Rev.*, 2000, **208**, 115; (*d*) R. C. Evans, P. Douglas and C. J. Winscom, *Coord. Chem. Rev.*, 2006, **250**(15–16), 2093; (*e*) W.-Y Wong, Z. He, S.-K So, K.-L Tong and Z. Lin, *Organometallics*, 2005, **24**, 4079; (*f*) D. N. Kozhevnikov, V. N. Kozhevnikov, M. Z. Shafikov, A. M. Prokhorov, D. W. Bruce and J. A. G. Williams, *Inorg. Chem.*, 2011, **50**, 3804–3815; (*g*) A. F. Rausch, U. V. Monkowius, M. Zabel and H. Yersin, *Inorg. Chem.*, 2010, **49**, 7818–7825; (*h*) J. Schneider, P. Du, X. Wang, W. W. Brennessel and R. Eisenberg, *Inorg. Chem.*, 2009, **48**, 1498–1506; (*i*) L. Murphy and J. A. G. Williams, *Top. Organomet. Chem.*, 2010, **28**, 75–111; (*j*) D. N. Kozhevnikov, V. N. Kozhevnikov, M. M. Ustinova, A. Santoro, D. W. Bruce, B. Koenig, R. Czerwieniec, T. Fischer, M. Zabel and H. Yersin, *Inorg. Chem.*, 2009, **48**, 4179–4189.

2 (*a*) W. Lu, V. A. Roy and C.-M. Che, *Chem. Commun.*, 2006, 3972–3974; (*b*) W. Lu, S. S.-Y Chui, K.-M Ng and C.-M Che, *Angew. Chem., Int. Ed.*, 2008, **47**, 4568–4572; (*c*) H. Yersin, G. Gliemann and U. Rössler, *Solid State Commun.*, 1977, **21**, 915–918; (*d*) S. C. F. Kui, S. S.-Y. Chui, C.-M. Che and N. Zhu, *J. Am. Chem. Soc.*, 2006, **128**, 8297–8309.

3 (*a*) S.-W. Lai, M. C.-W. Chan, T.-C. Cheung, S.-M. Peng and C.-M. Che, *Inorg. Chem.*, 1999, **38**, 4046–4055; (*b*) B. Ma, J. Li, P. I. Djurovich, M. Yousufuddin, R. Bau and M. E. Thompson, *J. Am. Chem. Soc.*, 2005, **127**, 28–29; (*c*) W. Lu, B.-X. Mi, M. C. W. Chan, Z. Hui, C.-M. Che, N. Zhu and S.-T. Lee, *J. Am. Chem. Soc.*, 2004, **126**, 4958.

4 (*a*) M. Albrecht, A. L. Spek and G. Van Koten, *J. Am. Chem. Soc.*, 2001, **123**, 7233–7246; (*b*) J. A. M. Van Beek, G. Van Koten, W. J. J. Smeets and A. L. Spek, *J. Am. Chem. Soc.*, 1986, **108**, 5010–5011; (*c*) R. A. Gossage, A. D. Ryabov, A. L. Spek, D. J. Stufkens, J. A. M. van Beek, R. van Eldik and G. van Koten, *J. Am. Chem. Soc.*, 1999, **121**, 2488–2497; (*d*) A. V. Zelewsky, A. P. Suckling and H. S. Evans, *Inorg. Chem.*, 1993, **32**, 4585–4593; (*e*) L. Chassot, A. V. Zelewsky, D. Sandrini, M. Maestri and V. Balzani, *J. Am. Chem. Soc.*, 1986, **108**, 6084–6085.

5 (*a*) S. H. Crosby, G. J. Clarkson and J. P. Rourke, *J. Am. Chem. Soc.*, 2009, **131**, 14142–14143; (*b*) M. Albrecht, *Chem. Rev.*, 2010, **110**, 576–623; (*c*) C. R. Baar, L. P. Carbray, M. C. Jennings, R. J. Puddephatt and J. J. Vittal, *Organometallics*, 2001, **20**, 408–417; (*d*) C. R. Baar, G. S. Hill, J. J. Vittal and R. J. Puddephatt, *Organometallics*, 1998, **17**, 32–40; (*e*) M. Crespo, M. Font-Bardia and X. Solans, *Organometallics*, 2004, **23**, 1708–1713; (*f*) C. M. Anderson, M. Crespo, M. C. Jennings, A. J. Lough, G. Ferguson and R. J. Puddephatt, *Organometallics*, 1991, **10**, 2672–2679.

6 S. W. Thomas, K. Venkatesan, P. Muller and T. M. Swager, *J. Am. Chem. Soc.*, 2006, **128**, 16641–16648.

7 (*a*) S. Jamali, S. M. Nabavizadeh and M. Rashidi, *Inorg. Chem.*, 2008, **47**, 5441–5452; (*b*) S. M. Nabavizadeh, M. G. Haghighi, A. R. Esmaeilbeig, F. Raoof, Z. Mandegani, S. Jamali, M. Rashidi and R. J. Puddephatt, *Organometallics*, 2010, **29**, 4893–4899; (*c*) M. G. Haghighi, M. Rashidi, S. M. Nabavizadeh, S. Jamali and R. J. Puddephatt, *Dalton Trans.*, 2010, **39**, 1–7; (*d*) S. M. Nabavizadeh, H. Amini, H. R. Shahsavari, M. Namdar, M. Rashidi and R. Kia, *Organometallics*, 2011, **30**, 1466–1477.

8 (*a*) J. C. M. Rivas and L. Brammer, *Inorg. Chem.*, 1998, **37**, 4756–4757; (*b*) M. Albrecht, P. Dani, M. Lutz, A. L. Spek and G. V. Koten, *J. Am. Chem. Soc.*, 2000, **122**, 11822–11833.

9 (*a*) G. R. Desiraju, *Crystal Design: Structure and Function*, 2003, **7**, John Wiley & Son; (*b*) L. Brammer, E. A. Bruton and P. Sherwood, *Cryst. Growth Des.*, 2001, **1**, 277–290.

10 (*a*) C. K. Lee, H. H. Peng and I. J. B. Lin, *Chem. Mater.*, 2004, **16**, 530–536; (*b*) U. Bentrup, M Feist and E. Kemnitz, *Prog. Solid State Chem.*, 1999, **27**, 75; (*c*) A. Bonamartini-Corradi, L. P. Battaglia, J. Rubenacker, R. D. Willett, T. E. Grigereit, P. Zhou and J. E. Drumheller, *Inorg. Chem.*, 1992, **31**, 3859; (*d*) M. J. Riley, D. Neill, P. V. Bernhardt, K. A. Byriel and C. H. L. Kennard, *Inorg. Chem.*, 1998, **37**, 3635; (*e*) M. V. Jiménez, J. J. Torrente, P. M. I. Gierz, F. J. Lahoz and L. A. Oro, *Organometallics*, 2008, **27**, 224–234; (*f*) D. V. Yandulov, K. G. Caulton, N. V. Belkova, E. S. Shubina, L. M. Epstein, D. V. Khoroshum, D. G. Musaev and K. Morokuma, *J. Am. Chem. Soc.*, 1998, **120**, 12553.

11 J. S. Miller and A. J. Epstein, *Prog. Inorg. Chem.*, 1976, **20**, 1.

12 K. Wiberg, *Tetrahedron*, 1968, **24**, 1083.

13 C. F. Matta, N. Castillo and R. J. Boyd, *J. Phys. Chem. B*, 2006, **110**, 563–578.
14 J. Brooks, Y. Babayan, S. Lamansky, P. I. Djurovich, I. Tsyba, R. Bau and M. E. Thompson, *Inorg. Chem.*, 2002, **41**, 3055–3066.
15 A. F. Rausch, H. H. H. Homeier and H. Yersin, *Top. Organomet. Chem.*, 2010, **29**, 193–235.
16 G. S. Hill, M. J. Irwin, C. J. Levy, L. M. Rendina and R. J. Puddephatt, *Inorg. Synth.*, 1998, **32**, 149.
17 J. S. Owen, J. A. Labinger and J. E. Bercaw, *J. Am. Chem. Soc.*, 2004, **126**, 8247.
18 R. C. Clark and J. S. Reid, *Acta Crystallogr., Sect. A: Found. Crystallogr.*, 1995, **51**, 887.
19 *Xcalibur CCD System: Absorption correction* (2006) CrysAlis-Software package, Oxford Diffraction Ltd.
20 A. Altomare, M. C. Burla, M. Camalli, G. L. Cascarano, C. Giacovazzo, A. Guagliardi, A. G. G. Moliterni, G. Polidori and R. Spagna, *J. Appl. Crystallogr.*, 1999, **32**, 115–119.
21 G. M. Sheldrick, *Acta Cryst.*, 2008, **A64**, 112–122.
22 Stoe & Cie (2005). X-AREA (Version 1.31), X-RED (Version 1.31) and XSHAPE(Version 2.05). Stoe & Cie, Darmstadt, Germany.

